

# Biofabricating Multifunctional Soft Matter with Enzymes and Stimuli-Responsive Materials

Yi Liu, Jessica L. Terrell, Chen-Yu Tsao, Hsuan-Chen Wu, Vishal Javvaji, Eunkyong Kim, Yi Cheng, Yifeng Wang, Rein V. Ulijn, Srinivasa R. Raghavan, Gary W. Rubloff, William E. Bentley, and Gregory F. Payne\*

Methods that allow soft matter to be fabricated with controlled structure and function would be beneficial for applications ranging from flexible electronics to regenerative medicine. Here, the assembly of a multifunctional gelatin matrix is demonstrated by triggering its self-assembly and then enzymatically assembling biological functionality. Triggered self-assembly relies on electrodeposition of the pH-responsive hydrogelator, 9-fluorenylmethoxycarbonyl-phenylalanine (Fmoc-Phe), in response to electrical inputs that generate a localized pH-gradient. Warm solutions of Fmoc-Phe and gelatin are co-deposited and, after cooling to room temperature, a physical gelatin network forms. Enzymatic assembly employs the cofactor-independent enzyme microbial transglutaminase (mTG) to perform two functions: crosslink the gelatin matrix to generate a thermally stable chemical gel and conjugate proteins to the matrix. To conjugate globular proteins to gelatin these proteins are engineered to have short lysine-rich or glutamine-rich fusion tags to provide accessible residues for mTG-catalysis. Viable bacteria can be co-deposited and entrapped within the crosslinked gelatin matrix and can proliferate upon subsequent incubation. These results demonstrate the potential for enlisting biological materials and mechanisms to biofabricate multifunctional soft matter.

is considerable interest in harnessing the properties of soft, and especially biological, materials to provide functional assemblies. Probably the most visible soft-matter fabrication activities are focused on regenerative and personalized medicine (e.g., tissue engineering and targeted drug delivery). However, advances in soft-matter fabrication could transform a broader range of activities: the integration of biological components into electronic devices will facilitate multiplexed analysis at the point-of-care and high-throughput drug discovery; the versatility and ease of processing of organic materials provides a low-cost platform for “smarter” paper, textiles and packaging; and the compatibility of many soft materials with biology allows opportunities for agriculture, foods and cosmetics.

The fabrication of soft matter can be enabled by biology which provides a suite of materials, mechanisms and insights. Self-assembly is the hallmark of biological

## 1. Introduction

The information age was enabled by microfabrication methods that allowed hard materials to be organized into assemblies that harnessed their electronic and optical properties. There

fabrication as information contained within the molecules themselves guide assembly over a hierarchy of length scales. Often, biological self-assembly enlists molecular-recognition and is triggered by external stimuli. Also, biology employs enzymes to recognize molecular information (e.g., an amino acid residue or

Dr. Y. Liu, Dr. E. Kim, Prof. W. E. Bentley, Prof. G. F. Payne  
Institute for Bioscience and Biotechnology Research  
University of Maryland  
5115 Plant Sciences Building  
College Park, MD 20742, USA  
E-mail: gpayne@umd.edu

J. L. Terrell, Dr. C.-Y. Tsao, Dr. H.-C. Wu, Prof. W. E. Bentley,  
Prof. G. F. Payne  
Fischell Department of Bioengineering  
University of Maryland  
College Park, MD 20742, USA  
V. Javvaji, Prof. S. R. Raghavan  
Department of Chemical and Biomolecular Engineering  
University of Maryland  
College Park, MD 20742, USA

Dr. Y. Cheng, Prof. G. W. Rubloff  
Institute for Systems Research and, Department  
of Materials Science and Engineering  
University of Maryland  
College Park, MD 20742, USA

Dr. Y. Wang  
School of Material Science and Engineering  
Wuhan University of Technology  
Wuhan, 430070, P. R. China  
Prof. R. V. Ulijn  
WestCHEM Department of Pure and Applied Chemistry  
The University of Strathclyde  
295 Cathedral Street, Glasgow G1 1XL, Scotland, UK



DOI: 10.1002/adfm.201200095

sequence) for the generation/cleavage of covalent bonds. Here, we report the biofabrication of multifunctional soft matter by the triggered self-assembly of stimuli-responsive materials and the enzymatic introduction of linkages to build macromolecular structure and function.

Electrodeposition is an attractive method for triggered self-assembly because it enlists the capabilities of electronics to impose electrical signals with exquisite spatial and temporal control.<sup>[1–4]</sup> Over the last decade, several stimuli-responsive biological polymers have been shown to respond to imposed electrical signals by undergoing a localized and reversible sol-gel transition.<sup>[5–11]</sup> To our knowledge, the reversible electrodeposition mechanisms that are currently known rely on pH gradients generated by electrolytic reactions. Here, we exploit the pH-responsive gel-forming properties of the small molecule hydrogelator<sup>[12–18]</sup> Fmoc-phenylalanine (Fmoc-Phe)<sup>[19–21]</sup> to co-deposit the thermally responsive protein gelatin. Gelatin is a gel-forming biopolymer that is widely used for food, pharmaceutical and food applications. We use Fmoc-Phe for co-deposition because no mechanisms are known for the direct electrodeposition of gelatin. After deposition and cooling, **Scheme 1a** shows that gelatin forms its physical (i.e., non-covalent) gel and Fmoc-Phe can be “leached” from the electrodeposited hydrogel.

The concept of enlisting enzymes for macromolecular construction is attractive because of the potential of catalyzing reactions selectively and under mild aqueous conditions. However, few enzymes are known that build macromolecular structure (vs cleavage) without requiring complex co-factors or activated substrates.<sup>[22–25]</sup> Here we enlist a co-factor-independent microbial transglutaminase (mTG) that catalyzes amide bond formation between lysine and glutamine residues of proteins.<sup>[26–28]</sup> As illustrated in **Scheme 1a**, we use mTG to covalently crosslink the electrodeposited gelatin hydrogel to impart thermal stability to this matrix.<sup>[29–34]</sup> Further, we employ mTG to bio-functionalize

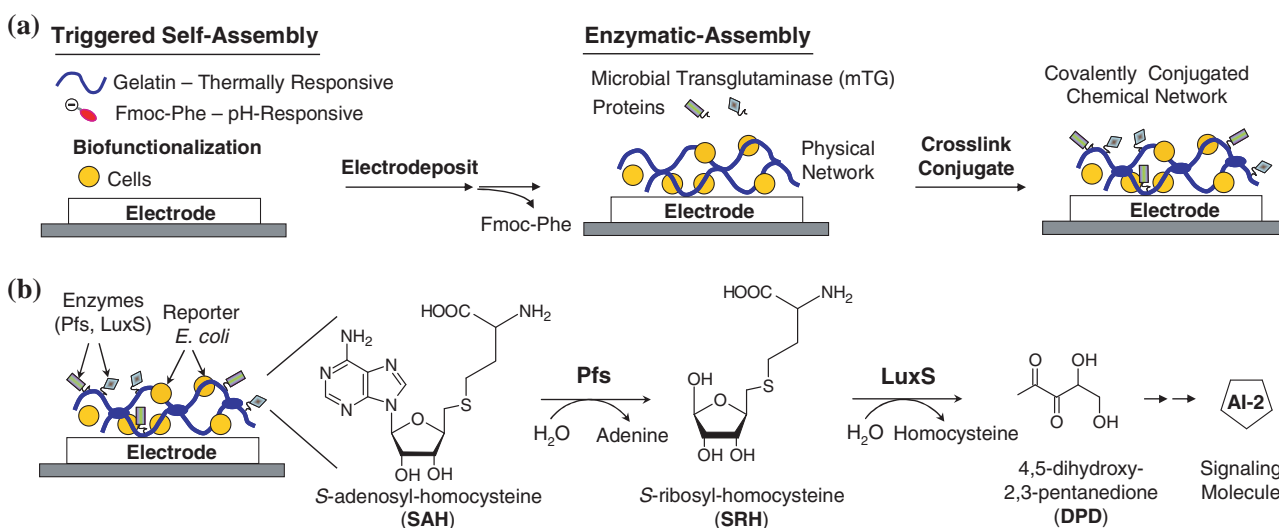
the hydrogel by anchoring globular proteins to the gelatin. Since amino acid residues of globular proteins are typically inaccessible for enzymatic reactions,<sup>[35]</sup> the proteins were engineered with lysine or glutamine fusion tags to provide the recognition site for enzymatic assembly.<sup>[36–41]</sup>

To demonstrate the potential for coupling triggered self-assembly (i.e., electrodeposition) with enzymatic-assembly, we biofabricated the functional matrix illustrated in **Scheme 1b**. Specifically, the matrix was functionalized by conjugating two enzymes (designated Pfs and LuxS) from a short bacterial pathway for the synthesis of a small signaling molecule. The matrix also contains entrapped reporter cells that respond to this in situ generated signaling molecule by switching-on the expression of a model fluorescent protein.

## 2. Results and Discussion

### 2.1. Triggered Self-Assembly of Gelatin (Electrodeposition)

In our initial study, we used rheology to examine the stimuli-responsive properties of the gelatin/Fmoc-Phe hybrid system. In the first experiment, a warm mixture of gelatin (5%) and Fmoc-Phe (0.3%) in the absence (control) or presence (sample) of HCl (2 mM) was prepared and loaded onto the rheometer stage that had been set to 30 °C. **Figure 1a** shows that when HCl was added to the gelatin/Fmoc-Phe solution, the elastic modulus ( $G'$ ) and viscous modulus ( $G''$ ) increased during the 85-min experiment. The increase in  $G''$  was faster than  $G'$ , and after 37 min,  $G'$  exceeded  $G''$  indicating the transition from solution to a gel. **Figure 1a** also shows that for the control (no HCl),  $G''$  remained considerably larger than  $G'$  throughout the experiment indicating that the control remained as a solution. This pH induced sol-gel transition is characteristic of Fmoc-Phe<sup>[19]</sup> and other Fmoc-peptide hydrogelators.<sup>[13,15,16]</sup>



**Scheme 1.** Biofabrication of multifunctional soft matter. a) Schematic illustrating the coupling of triggered self-assembly (i.e., electrodeposition) and enzymatic-assembly. b) Schematic illustrating that conjugated enzymes (Pfs and LuxS) allow for in situ generation of a bacterial signaling molecule (AI-2) that is detected by entrapped reporter cells.

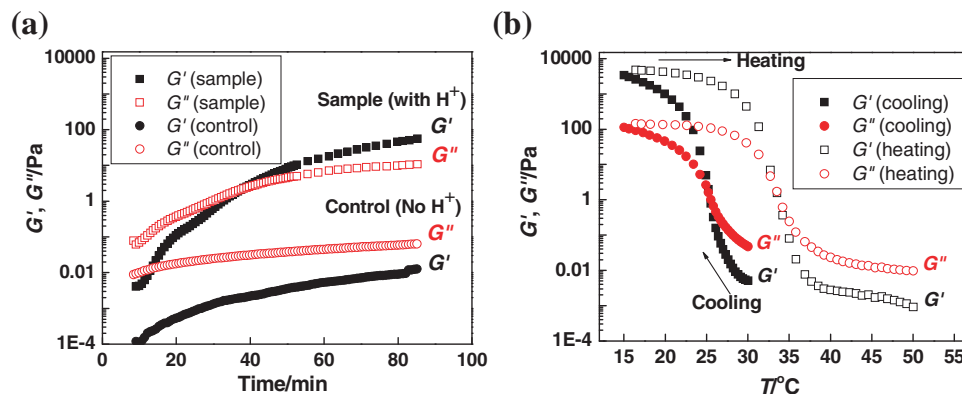


**Figure 1.** Orthogonal stimuli can trigger hydrogel self-assembly. a) Rheological evidence that gelatin (5%) and Fmoc-Phe (0.3%) can undergo gel formation (30 °C) by the addition of acid that reduces the pH from 7.5 to 6.0. b) Rheological evidence that gelatin/Fmoc-Phe undergoes a thermally reversible sol-gel transition upon cooling (pH = 7.5). In both cases, oscillatory strains (5%) were applied at 0.1 Hz.

Next we studied the thermally reversible behavior of the gelatin/Fmoc-Phe system. In this experiment, the warm mixture was loaded onto the rheometer stage (30 °C) and equilibrated for 10 min. Then the temperature was lowered from 30 to 15 °C ( $\approx 0.43$  °C/min). After cooling, the sample was equilibrated at 15 °C for 20 min, and then the temperature was increased from 15 to 50 °C ( $\approx 0.53$  °C/min). Figure 1b shows that the gelatin and Fmoc-Phe mixture was initially a solution ( $G'' > G'$ ). When the temperature was lowered below 25 °C the sample transitioned from a sol to a gel (i.e.,  $G'$  became larger

than  $G''$ ). During heating, the gel was melted when the temperature was raised above 35 °C. The gelation and melting behavior in Figure 1b is characteristic of gelatin,<sup>[42,43]</sup> indicating that the addition of Fmoc-Phe has little effect on this thermally-reversible behavior. The rheological measurements of Figure 1 demonstrate that Fmoc-Phe confers pH-responsive behavior while gelatin confers thermal-responsive behavior.

The pH-responsive gel-forming behavior of Fmoc-Phe<sup>[20,21,44]</sup> allows it to co-deposit gelatin as depicted in Figure 2a. The low pH generated at the anode induces Fmoc-Phe to undergo

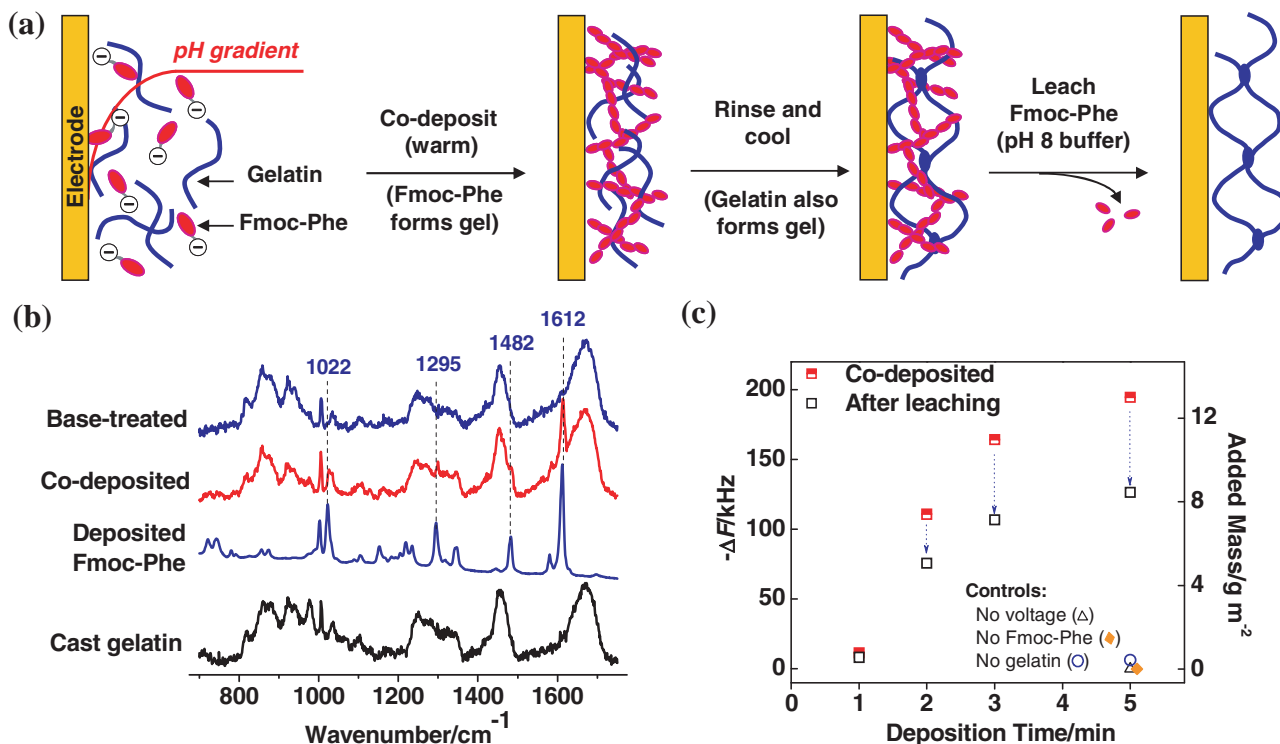


**Figure 2.** Co-deposition of gelatin using Fmoc-Phe. a) Schematic illustrating experimental procedure for gelatin co-deposition. b) Chemical (Raman) evidence that gelatin can be co-deposited and Fmoc-Phe can be “leached” from the gelatin hydrogel. c) Physical (ex situ QCM) evidence for co-deposition and Fmoc-Phe removal.

a localized sol-gel transition that entraps unstructured gelatin chains. Upon cooling, the gelatin chains undergo a separate sol-gel transition. After gelatin forms its gel network, the Fmoc-Phe can be removed by treating the deposited hydrogel with pH 8 buffer that disrupts the Fmoc-Phe network<sup>[45]</sup> and allows the Fmoc-Phe to be leached from the gelatin hydrogel.<sup>[20]</sup>

The co-deposition of gelatin/Fmoc-Phe was demonstrated using a gold-coated silicon wafer (i.e., chip). In this experiment, the chip was partially immersed in a warm deposition solution (37 °C) containing gelatin (5%), Fmoc-Phe (0.3%), hydroquinone (50 mM), and NaCl (50 mM), and then the gold was biased to serve as the anode (0.5 A m<sup>-2</sup>) and a platinum wire was used as the cathode. Hydroquinone was included in the deposition solution to enable the pH gradient to be generated at lower anodic potentials and thus limit damage to the gold chip.<sup>[21,44,46]</sup> After 4 min deposition, the chip was removed from the deposition solution and gently rinsed with cool water. The wet hydrogel film was visually observed to adhere to the electrode surface, and after drying in air at room temperature (22 °C), the thickness was measured by profilometry to be 4.4 μm.

Chemical evidence for co-deposition was provided by Raman spectroscopy. The bottom two spectra in Figure 2b are controls that show characteristic peaks for gelatin and Fmoc-Phe.<sup>[20,47–49]</sup> The spectrum for the co-deposited hydrogel film shows peaks for both gelatin and Fmoc-Phe, providing direct evidence that Fmoc-Phe allows for the co-deposition of gelatin. The co-deposited film was then treated with pH 8 buffer for 15 min to leach Fmoc-Phe from the network and the Raman spectrum of this film indicates that the characteristic peaks of Fmoc-Phe have disappeared, whereas the characteristic peaks of gelatin are retained. This result provides direct chemical evidence that Fmoc-Phe can be removed from the co-deposited hydrogel network.

Physical evidence for gelatin/Fmoc-Phe co-deposition is provided by ex situ QCM measurements. Similar to the experimental procedure described above, a gold-coated QCM crystal was immersed in the deposition solution; a constant anodic current (0.5 A m<sup>-2</sup>) was applied to the gold electrode for a specific time; the crystal was removed from the solution, washed with cool water, and vacuum dried at room temperature for 2 h; and then the resonance frequency was measured and compared to the initial frequency measured before deposition.

Separate crystals were used for each deposition-time measurement. The ex situ QCM results in Figure 2c show an increase in frequency shift ( $-\Delta F$ ) with deposition time for up to 5 min. Longer deposition times were not studied because the deposited mass exceeded the instrument's measurement limits. The scale at the right in Figure 2c is the mass of the deposited film and this estimate was obtained using the Sauerbrey equation to convert the frequency change to mass of the dried film.<sup>[46,50]</sup> The three controls shown at the lower right in Figure 2c are the measurements in the absence of voltage, Fmoc-Phe, or gelatin. No deposition was observed for either the "no voltage" or "no Fmoc-Phe" control. A small amount of mass (0.4 g m<sup>-2</sup>) was deposited for the "no gelatin" control and this value was comparable to the mass of electrodeposited Fmoc-Phe reported in previous studies.<sup>[21]</sup> Interestingly, the amount of gelatin co-deposited by Fmoc-Phe is considerably larger than the amount of agarose that was co-deposited by Fmoc-Phe observed in previous studies<sup>[20]</sup> (8.4 vs. 0.2 g m<sup>-2</sup> at 5 min under similar conditions). These QCM results indicate that Fmoc-Phe is required for electrodeposition and that deposition can be controlled by deposition conditions (e.g., deposition time).

In addition to studying deposition, we used QCM to provide physical evidence for the removal of Fmoc-Phe from the deposited hydrogel. After measuring the frequency shift for the dried films after deposition, the QCM crystals were incubated in pH 8 buffer for 15 min, rinsed, dried, and re-measured by QCM. As illustrated by the arrows in Figure 2c, a decrease of frequency change was observed for each of the film-coated crystals, consistent with the removal of Fmoc-Phe from the deposited film. Thus, the results in Figure 2 demonstrate that the pH-responsive Fmoc-Phe can serve as a temporary fabrication scaffold for the electrodeposition of the thermally-responsive gelatin.

## 2.2. Enzymatic Crosslinking and Conjugation

The first function of transglutaminase (mTG) is to covalently crosslink gelatin to create a thermally-stable network. To demonstrate crosslinking, we performed rheological measurements at 30 °C with a solution of gelatin (5%), Fmoc-Phe (0.3%), and mTG (15 U g<sup>-1</sup> gelatin). Figure 3a shows that when mTG was

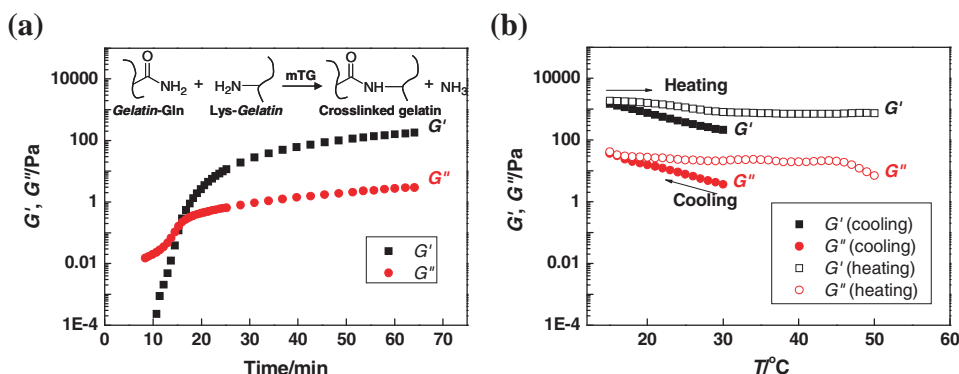


**Figure 3.** Enzymatic crosslinking of gelatin to confer thermal stability. a) Rheological evidence that microbial transglutaminase (mTG; 15 U g<sup>-1</sup> gelatin) catalyzes a sol-gel transition for a warm sample (30 °C; 5% gelatin; 0.3% Fmoc-Phe). b) Temperature sweep demonstrates that the mTG-crosslinked hydrogel is thermally stable and no longer undergoes reversible sol-gel transitions.

added to the gelatin/Fmoc-Phe solution,  $G'$  and  $G''$  increased dramatically during the 65-min experiment. The increase in  $G'$  was more rapid than  $G''$ , and after 16 min, Figure 3a shows that  $G'$  exceeded  $G''$ . These results provide rheological evidence that mTG catalyzes gel formation.<sup>[33,34,51]</sup>

To demonstrate that the mTG-crosslinked gelatin gel is thermally-stable, we measured its rheological properties as a function of temperature. Figure 3b shows that initially, the crosslinked network is a gel ( $G' > G''$ ) and both moduli increased when the gel was cooled to 15°C. Upon subsequent heating,  $G'$  and  $G''$  of the crosslinked gel remained nearly constant with  $G'$  remaining substantially greater than  $G''$  indicating that this gel did not return to a solution at the increased temperatures. These results demonstrate that mTG-crosslinking confers thermal stability to the gelatin network.

The second function of mTG is to conjugate proteins to the gelatin matrix. To demonstrate mTG-conjugation of globular proteins we used model fluorescent proteins. Several studies indicate that amino acid residues of globular proteins are not accessible for enzymatic conjugation and thus globular proteins are typically engineered to have lysine-rich or glutamine-rich fusion tags to facilitate mTG-catalyzed conjugation.<sup>[36–41]</sup> For our studies, we engineered the enhanced green fluorescent protein to have a C-terminal tag with 7 added lysine residues (Lys-EGFP), and the red fluorescent protein to have an N terminal tag with 5 added glutamine residues (Gln-RFP).

To demonstrate mTG-conjugation, we performed the experiment illustrated in Figure 4a. Initially gelatin was co-deposited with Fmoc-Phe onto a patterned gold electrode and then the chip was incubated with mTG (0.5 U mL<sup>-1</sup>) and either Lys-EGFP or Gln-RFP (20 μg mL<sup>-1</sup>). After reacting overnight, the chip was rinsed with phosphate buffered saline (PBS; pH 7.4) and examined using fluorescence microscopy. As indicated by the left images in Figure 4b,c, the Lys-EGFP and Gln-RFP were both assembled onto the gelatin film that was spatially localized on the gold electrode. Since mTG can simultaneously conjugate and crosslink gelatin, we expect the treated gelatin film to be thermally stable. Thermal stability was tested by incubating the

chips in warm water (37 °C) for 2 h. The images at the right in Figure 4b,c show no change in fluorescence intensity for the mTG-treated films while the control films without mTG treatment were observed to dissolve upon incubation in warm water. Thus, mTG can simultaneously crosslink gelatin and conjugate proteins to this protein matrix.

### 2.3. On-Chip Bacterial Entrapment and Cultivation

Both electrodeposition and enzymatic-crosslinking are performed under mild conditions that should allow viable populations to be co-deposited and entrapped within the hydrogel matrix. To test this possibility, we co-deposited and cultured entrapped *E. coli* cells. For this experiment the bacteria were initially cultured in LB medium to an OD<sub>600</sub> of 4.0, 0.35 mL of this cell suspension was centrifuged, the pellet was re-suspended with 50 μL PBS buffer and added to 6 mL deposition solution containing gelatin (5%) and Fmoc-Phe (0.3%). Deposition was performed using an ITO-coated glass slide. ITO is more stable than gold under the anodic potentials (~2.4 V) and thus hydroquinone was not necessary for deposition onto the ITO-coated slide. Also, the ITO coating is transparent and allows optical measurements to be used to monitor growth of the entrapped cell population.

As schematically illustrated in Figure 5a, an ITO-coated glass slide was partially immersed in the deposition solution at 37 °C and an anodic voltage was applied to a current density of 0.1 A m<sup>-2</sup> for 30 min. (A lower current density was used for ITO slide to maintain a voltage less than 2.4 V.) After deposition, the film was rinsed with cool water, briefly incubated in air (~10 min) to allow the hydrogel to “set”, and then incubated for 1 h in 20 mM PBS buffer (pH 7.4) containing mTG (1 U mL<sup>-1</sup>) to crosslink the gelatin. The cell-containing film was then rinsed and incubated in LB medium at 37 °C, and the optical density was measured intermittently.

The growth curve in Figure 5b shows a steady increase in optical density for the gels, while a control film electrodeposited

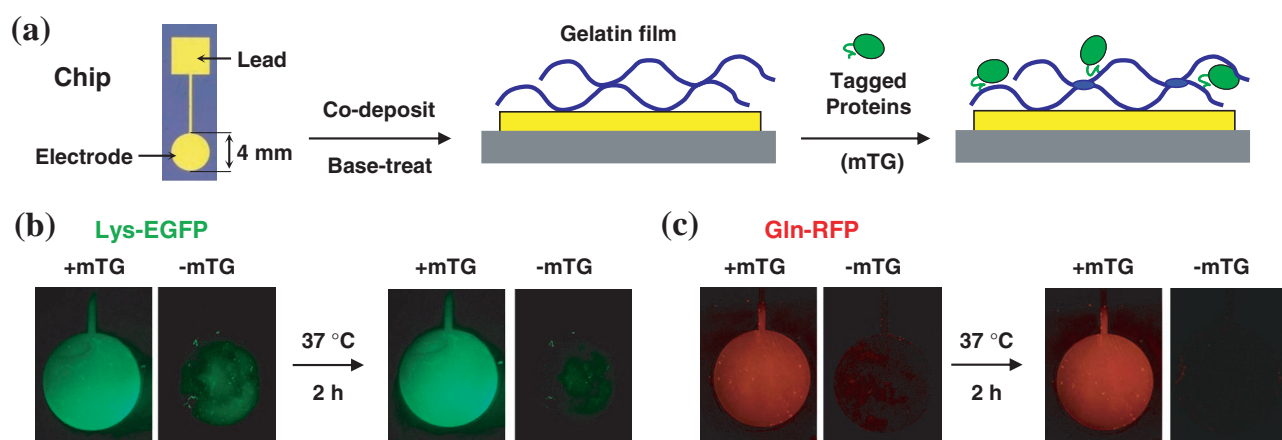


**Figure 4.** Enzymatic conjugation of fusion-tagged proteins to electrodeposited gelatin. a) Schematic illustrating experimental procedure. b) Fluorescence images of electrode address in which transglutaminase (mTG; 0.5 U mL<sup>-1</sup>) simultaneously crosslinked and conjugated Lys-EGFP (20 μg mL<sup>-1</sup>) to the electrodeposited gelatin. c) Fluorescence images of electrode address in which mTG (0.5 U mL<sup>-1</sup>) crosslinked and conjugated Gln-RFP (20 μg mL<sup>-1</sup>) to the electrodeposited gelatin.

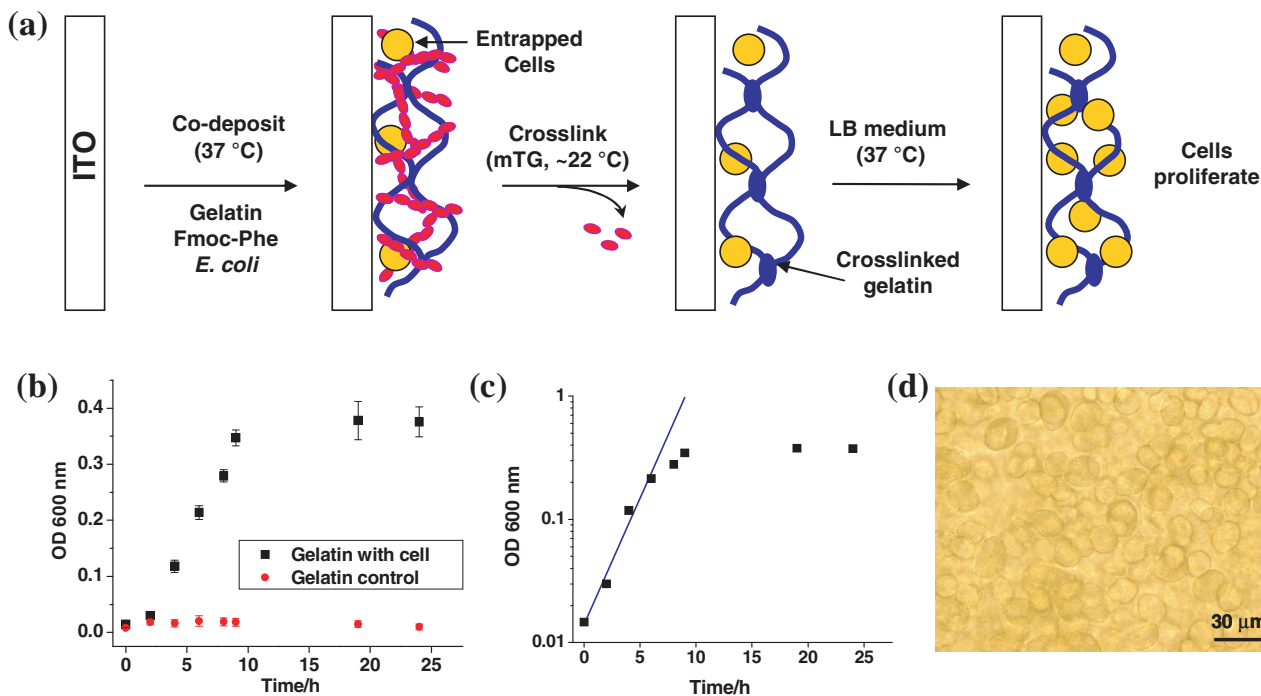


**Figure 5.** Co-deposition, entrapment and cultivation of *E. coli* in a crosslinked gelatin matrix. a) Schematic illustrating experimental procedure. b) Growth curve as measured by optical density for cells incubated at 37 °C. c) Semilogarithmic plot of growth suggesting exponential growth occurs with a doubling time 1.5 h. d) Bright-field image of entrapped cell colonies (~20 μm) after incubation for 18 h in the gelatin gel.

without cells shows no change in optical density. The semi-logarithmic plot in Figure 5c suggests the entrapped population undergoes exponential growth for about 6 h with a doubling time of 1.5 h. The bright field image in Figure 5d was obtained after incubating the cells for 18 h in the gelatin gel. This image indicates that cell growth is accompanied by the appearance of ~20 μm colonies. Presumably colonies are formed because of the restricted mobility of the cells within the gel network (e.g., the cells can divide but the daughter cells are physically constrained by the network and cannot readily move away). Colony-type growth was observed in previous studies when *E. coli* was co-deposited and cultured in alginate gels.<sup>[7,52]</sup> The results in Figure 5 indicate that electrodeposition and enzymatic-crosslinking enable a viable bacterial population to be assembled and cultivated “on-chip”.

#### 2.4. In-film Processing for Cell Signaling and Biosensing

As a proof-of-concept, we biofabricated a multifunctional gelatin-based matrix capable of generating and reporting a bacterial quorum sensing signaling molecule. Bacterial communities communicate through small signaling molecules that can induce population-dependent changes in gene expression and phenotypic behavior (e.g., biofilm formation).<sup>[53–61]</sup> Because quorum sensing has been implicated in bacterial pathogenesis there have been recent studies to generate inhibitory small molecules<sup>[62–68]</sup> and materials<sup>[69,70]</sup> as a means to control infections. Here, we examined the quorum sensing based on the autoinducer 2 (AI-2) signaling molecule in *E. coli*. As illustrated in

Scheme 1b, AI-2 is synthesized in a two-step pathway involving the enzymes Pfs and LuxS.

For our proof-of-concept demonstration, we engineered the Pfs and LuxS enzymes to have C terminal tags (either 7 Lys or 5 Gln) to facilitate mTG-catalyzed conjugation to the gelatin matrix. These conjugated enzymes functionalized the matrix to synthesize the AI-2 signaling molecule. The in situ generated AI-2 was detected using entrapped reporter cells [CT104 (pCT6 + pET200-DsRed)]<sup>[71–73]</sup> that had been engineered to express the model fluorescent protein (DsRed)<sup>[74]</sup> upon exposure to AI-2. Details of the molecular biology are provided in the Supporting Information.

**Figure 6a** illustrates the experimental approach for biofabricating the multifunctional matrix. First, 0.1 mL of a reporter cell suspension was added to 6 mL deposition solution containing gelatin (5%) and Fmoc-Phe (0.3%). Next, this cell-containing solution was electrodeposited onto an ITO-coated glass slide by partially immersing it in the deposition solution at 37 °C and applying an anodic potential (0.1 A m<sup>-2</sup>) for 15 min. After rinsing with cool water and incubating in air to allow the hydrogel to set, the deposited film was crosslinked/conjugated by incubating for 2 h in PBS containing mTG (1.5 U mL<sup>-1</sup>) and the “fusion-tagged” Pfs and LuxS enzymes (100 μg mL<sup>-1</sup>). Control samples were prepared by deleting one or both enzymes from the reaction mixture. These bio-functionalized films were then incubated in LB medium at 37 °C for 1 h to permit cell recovery. Finally, the films were transferred to a 50 mM tris buffer solution (with 10% v/v LB medium) containing the precursor SAH (0.9 mM) and incubated at 37 °C for 18 h.

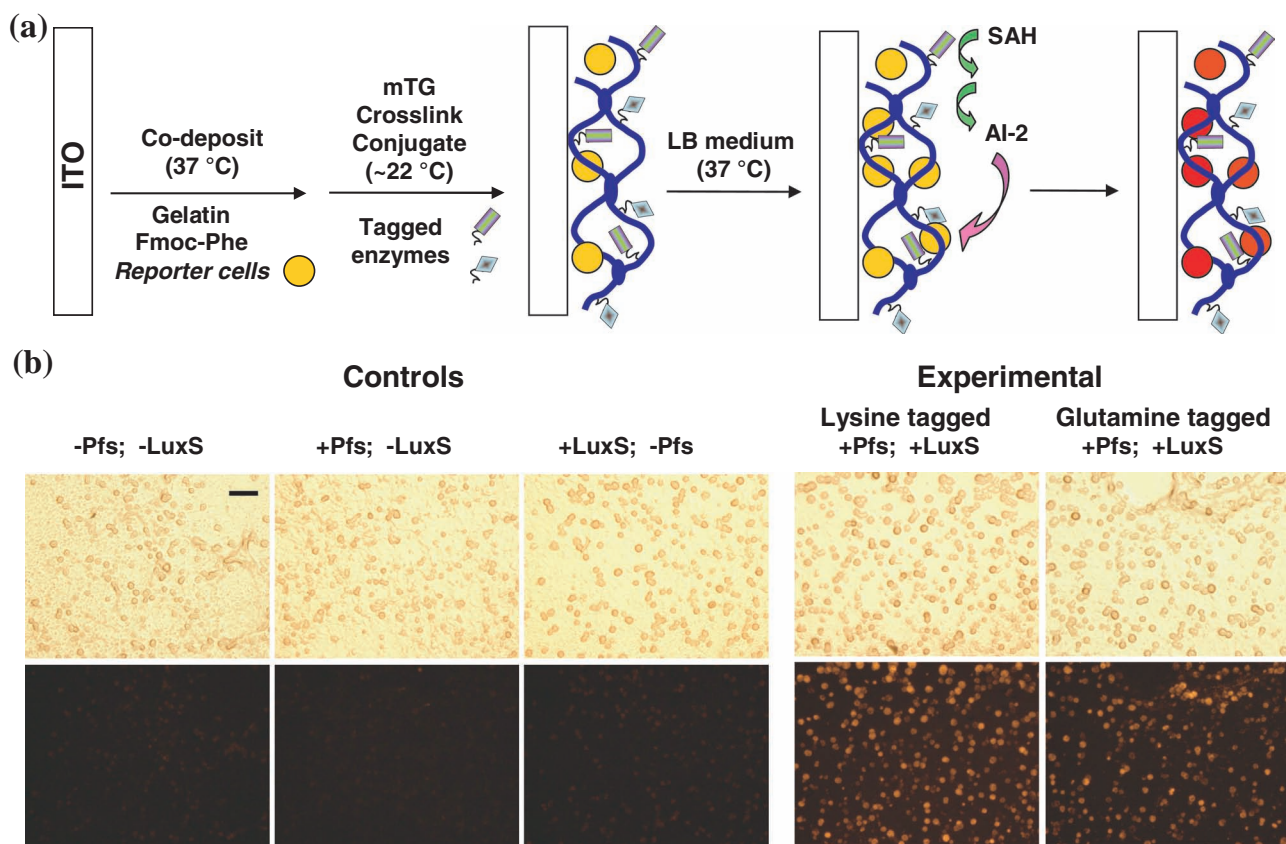


**Figure 6.** Multifunctional gelatin-based matrix capable of in situ synthesis and detection of a bacterial quorum sensing signaling molecule. a) Schematic showing the enzymatic assembly of two components (Pfs and LuxS) of a bacterial pathway to synthesize autoinducer 2 (AI-2) on the same gelatin matrix with entrapped reporter cells. b) Bright-field and fluorescence images showing the response of entrapped reporter cells after 18 h incubation (37 °C) with precursor (SAH). Three controls were prepared lacking one or both of the Pfs/LuxS biosynthetic enzymes while two samples were prepared using Pfs/LuxS enzymes tagged with either lysine-rich or glutamine-rich fusion tags. Scale bar = 100  $\mu\text{m}$ .

The bright field images in Figure 6b shows that the entrapped *E. coli* grew in colonies in all samples during the course of the experiment. The fluorescence images at the bottom left in Figure 6b show that the three control samples show very weak fluorescence, indicating that the entrapped reporter cells were not induced. This result is expected since the control matrices lacked one or both of the AI-2 synthetic enzymes. The right two fluorescence images in Figure 6b show considerable fluorescence. These results are also expected because these two matrices are functionalized with both the Pfs and LuxS synthetic enzymes (the enzymes possessed either Lys or Gln fusion tags).

The results in Figure 6 demonstrate that enzymatic conjugation allows the reconstitution of this biosynthetic pathway and the in situ generation of the AI-2 signaling molecule. Further, the AI-2 can diffuse through the matrix to access the entrapped cells which are induced to express genes from the inducible promoter. While the goal of this study was to demonstrate the construction of a multifunctional matrix, the results suggest potential applications. For instance, this biofunctionalized matrix may provide a platform to screen drugs capable of inhibiting AI-2 synthesis. Such inhibitors might disrupt processes that are mediated by quorum sensing such as biofilm formation<sup>[60,61,75,76]</sup> or pathogenesis.<sup>[77–80]</sup>

### 3. Conclusions

We demonstrate the coupling of triggered self-assembly and enzymatic-assembly for the spatially-controlled and hierarchical assembly of multifunctional soft matter. Specifically, we use two self-assembling materials that can be triggered to undergo reversible sol-gel transitions in response to orthogonal stimuli. Fmoc-Phe forms a gel upon reducing the pH and serves as a temporary fabrication aid that allows electrodeposition of gelatin. Gelatin is a biologically-friendly material that undergoes physical gel formation when the temperature is reduced. The enzyme microbial transglutaminase (mTG) serves two functions: it covalently-crosslinks the gelatin hydrogel to confer thermal stability to this matrix and it conjugates globular proteins to confer bio-functionality (e.g., enzymatic activity) to the matrix. Both gelatin's self-assembly and mTG's enzymatic-crosslinking/conjugation rely on molecular recognition to form the physical and chemical associations required for matrix fabrication; as a result reactive reagents are not required for assembly and protection/de-protection steps are unnecessary to confer selectivity to assembly. Thus the coupling of self- and enzymatic- assembly provides a simple, rapid and bio-friendly means to confer functionality to soft matter.

To illustrate the potential of this biofabrication approach, we functionalized a gelatin matrix with entrapped reporter cells and two pathway enzymes for the synthesis of a bacterial signaling molecule. We demonstrate that the matrix can convert the precursor into the signaling molecule which then induces gene expression in the entrapped reporter cells. In essence, this matrix “recognizes” chemical information from the external environment (the presence of the precursor) and transduces it into an optical output (expression of a fluorescent protein). Potentially, this biofunctionalized matrix could be used for analysis or the discovery of inhibitors that can disrupt this biological signaling process. More broadly, this work suggests the potential of biofabrication to organize and functionalize soft matter for a diverse range of applications.

#### 4. Experimental Section

**Materials:** The following materials were purchased from Sigma-Aldrich; gelatin from porcine skin (type A), Fmoc-D-phenylalanine (Fmoc-Phe,  $\geq 98\%$ ), DMSO (99.94%), hydroquinone (HQ,  $\geq 99\%$ ), sodium chloride (99.5+%), S-adenosylhomocysteine (SAH), phosphate buffered saline (PBS) tablets, and ITO-coated glass slides (surface resistivity  $\sim 30\text{--}70 \Omega/\text{sq}$ ). Sodium hydroxide ( $\geq 98.6\%$ ) and hydrochloric acid (37.8%) were purchased from Fisher Scientific. Microbial transglutaminase (mTG; Activa TI;  $100 \text{ U g}^{-1}$  as reported by the manufacturer) was obtained from Ajinomoto (Japan). Water was de-ionized with Millipore SUPER-Q water system until final resistivity  $> 18 \text{ M}\Omega\text{-cm}$  was reached.

**Solutions:** An Fmoc-Phe solution was prepared by; first dissolving Fmoc-Phe in DMSO ( $100 \text{ mg mL}^{-1}$ ), vortex-mixing this concentrate in water (with or without  $50 \text{ mM NaCl}$ , see text for details), then adding  $0.5 \text{ M NaOH}$  to dissolve. The solution was adjusted to a pH of 7.5 and filtered using a syringe filter. Hydroquinone was dissolved in the Fmoc-Phe solution when deposition was performed with gold electrode to lower the deposition voltage and reduce damage to the electrode. A gelatin stock solution (10%) was prepared by dissolving gelatin in  $4 \text{ mM NaOH}$  with or without  $50 \text{ mM NaCl}$  ( $50 \text{ mM}$ ) at  $65 \text{ }^\circ\text{C}$  and then equilibrating this solution in a  $37 \text{ }^\circ\text{C}$  incubator. The gelatin/Fmoc-Phe solutions were prepared by mixing corresponding amount of solutions of gelatin and Fmoc-Phe in a  $37 \text{ }^\circ\text{C}$  incubator. In cell studies, the bacteria cells were initially cultured in LB medium to an  $\text{OD}_{600}$  of 4.0. Before depositing,  $0.5\text{-mL}$  cell solution was centrifuged; the pellet was re-suspended with  $50 \mu\text{L}$  PBS buffer; mixed with  $3 \text{ mL}$  10% gelatin, and then mixed with  $3 \text{ mL}$  0.6% Fmoc-Phe. In initial studies, we observed that hydroquinone, but not Fmoc-Phe, inhibited bacterial growth and thus, hydroquinone and NaCl were not used when bacteria were co-deposited. For bacterial co-deposition we used an ITO-coated slide.

**Biofabrication Methods:** Electrodeposition was performed using gold-coated silicon wafers (designated “chips”) that were prepared and patterned by standard photolithographic methods as described elsewhere.<sup>[81]</sup> Before use, the gold electrodes were cleaned by immersing the chips in piranha solution (7:3 concentrated  $\text{H}_2\text{SO}_4$ :30%  $\text{H}_2\text{O}_2$ ) for 5 min. *Caution: piranha solution is a highly reactive mixture and results in a severely exothermic reaction. It should be kept out of contact with oxidizable organic materials.* Electrodeposition was performed in an incubator ( $\sim 37 \text{ }^\circ\text{C}$ ) using a DC power supply (2400 Sourcemeter, Keithley). First, the chips were partially-immersed in the reaction solution, and the electrode was biased to serve as the anode while a platinum wire served as cathode. After electrodeposition, the chip was removed from the deposition solution, rinsed with cool water, and dried at room temperature ( $22 \text{ }^\circ\text{C}$ ). Enzymatic crosslinking and conjugation were performed at room temperature. Crosslinking of the gelatin film was performed by immersing the chip into a PBS solution containing mTG ( $0.5\text{--}1.5 \text{ U mL}^{-1}$ ) for 1–2 h. Target proteins were conjugated to the electrodeposited gelatin by immersing the chip in a PBS buffer containing fusion tagged protein(s) and the reaction was initiated by adding mTG ( $1 \text{ U mL}^{-1}$ ).

**Molecular Biology:** The target proteins used in this study were engineered with lysine or glutamine fusion tags to facilitate mTG-catalyzed conjugation to the gelatin matrix. Specifically, we engineered the enhanced green fluorescent protein to have a C-terminal tag with 7 added lysine residues (Lys-EGFP), and the red fluorescent protein to have an N terminal tag with 5 added glutamine residues (Gln-RFP). We also engineered the enzymes, Pfs and LuxS, to have C terminal tags (either 7 Lys or 5 Gln). Methods to engineer these fusion tagged proteins are provided in Supporting Information. In this study, we use a reporter cell CT104 (pCT6 + pET200-DsRed) which is *luxS* and *IsrFG* double knockout strain that can sense extracellular signaling molecules and induce expression of the fluorescent protein (DsRed).<sup>[74]</sup>

**Instrumentation:** Rheological measurements were performed on a Rheometrics AR2000 stress-controlled rheometer (TA Instruments). A cone-and-plate geometry of 40 mm diameter and  $2^\circ$  cone angle was used with a solvent trap to prevent drying. Typically, oscillatory strains of 5% (which is within the linear viscoelastic regime) were applied at 0.1 Hz. Raman spectra were obtained from a Jobin Yvon LabRamHR Raman microscope. Ex situ quartz crystal microbalance (QCM) measurements of dried films were made with a CHI420a Electrochemical Analyzer (CH Instruments, Inc., Austin, TX) as described elsewhere.<sup>[82]</sup> The QCM crystal (ICM, Oklahoma City, OK) was placed in a humidity-controlled chamber (RH = 19%) and equilibrated for 10 min before frequency measurements. Optical density at 600 nm ( $\text{OD}_{600}$ ) was measured using a Thermo Scientific Evolution 60 spectrophotometer. Fluorescence on the chips was examined using an Olympus MVX10 MacroView microscope, and cell-containing samples were examined using an Olympus BX60 microscope. Images were obtained using an Olympus DP72 digital camera connected to the fluorescence microscope.

#### Supporting Information

Supporting Information is available from the Wiley Online Library or from the author.

#### Acknowledgements

The authors gratefully acknowledge financial support from the Robert W. Deutsch Foundation, the National Science Foundation (NSF; EFRI-0735987), and the Department of Defense, Defense Threat Reduction Agency (W91B9480520121) and the Office of Naval Research (N000141010446). They acknowledge the Maryland NanoCenter and its FabLab for the chip fabrication. The authors thank Dr. Xiaohua Yang for preparing the Gln-RFP.

Received: January 11, 2012

Revised: March 19, 2012

Published online: April 19, 2012

- [1] I. Zhitomirsky, A. Petric, *Am. Ceram. Soc. Bull.* **2001**, *80*, 41.
- [2] A. R. Boccaccini, S. Keim, R. Ma, Y. Li, I. Zhitomirsky, *J. R. Soc. Interface* **2010**, *7*, S581.
- [3] Y. Liu, E. Kim, R. Ghodssi, G. W. Rubloff, J. N. Culver, W. E. Bentley, G. F. Payne, *Biofabrication* **2010**, *2*, 022002.
- [4] S. T. Koev, P. H. Dykstra, X. Luo, G. W. Rubloff, W. E. Bentley, G. F. Payne, R. Ghodssi, *Lab Chip* **2010**, *10*, 3026.
- [5] M. Cheong, I. Zhitomirsky, *Colloid Surf. A-Physicochem. Eng. Asp.* **2008**, *328*, 73.
- [6] X. Pang, I. Zhitomirsky, *Mater. Chem. Phys.* **2005**, *94*, 245.
- [7] X. W. Shi, C. Y. Tsao, X. H. Yang, Y. Liu, P. Dykstra, G. W. Rubloff, R. Ghodssi, W. E. Bentley, G. F. Payne, *Adv. Funct. Mater.* **2009**, *19*, 2074.
- [8] L. Q. Wu, A. P. Gadre, H. M. Yi, M. J. Kastantin, G. W. Rubloff, W. E. Bentley, G. F. Payne, R. Ghodssi, *Langmuir* **2002**, *18*, 8620.

- [9] X. H. Yang, E. Kim, Y. Liu, X. W. Shi, G. W. Rubloff, R. Ghodssi, W. E. Bentley, Z. Pancer, G. F. Payne, *Adv. Funct. Mater.* **2010**, *20*, 1645.
- [10] T. Jiang, Z. Zhang, Y. Zhou, Y. Liu, Z. W. Wang, H. Tong, X. Y. Shen, Y. N. Wang, *Biomacromolecules* **2010**, *11*, 1254.
- [11] R. Ma, R. F. Epand, I. Zhitomirsky, *Colloid Surf. B-Biointerfaces* **2010**, *77*, 279.
- [12] D. J. Adams, *Macromol. Biosci.* **2011**, *11*, 160.
- [13] L. Chen, J. Raeburn, S. Sutton, D. G. Spiller, J. Williams, J. S. Sharp, P. C. Griffiths, R. K. Heenan, S. M. King, A. Paul, S. Fuzzeland, D. Atkins, D. J. Adams, *Soft Matter* **2011**, *7*, 9721.
- [14] R. V. Ulijn, A. M. Smith, *Chem. Soc. Rev.* **2008**, *37*, 664.
- [15] V. Jayawarna, M. Ali, T. A. Jowitt, A. E. Miller, A. Saiani, J. E. Gough, R. V. Ulijn, *Adv. Mater.* **2006**, *18*, 611.
- [16] R. Orbach, L. Adler-Abramovich, S. Zigerson, I. Mironi-Harpaz, D. Seliktar, E. Gazit, *Biomacromolecules* **2009**, *10*, 2646.
- [17] W. Helen, P. de Leonardis, R. V. Ulijn, J. Gough, N. Tirelli, *Soft Matter* **2011**, *7*, 1732.
- [18] C. Tang, A. M. Smith, R. F. Collins, R. V. Ulijn, A. Saiani, *Langmuir* **2009**, *25*, 9447.
- [19] S. Sutton, N. L. Campbell, A. I. Cooper, M. Kirkland, W. J. Frith, D. J. Adams, *Langmuir* **2009**, *25*, 10285.
- [20] Y. Liu, Y. Cheng, H. C. Wu, E. Kim, R. V. Ulijn, G. W. Rubloff, W. E. Bentley, G. F. Payne, *Langmuir* **2011**, *27*, 7380.
- [21] Y. Liu, E. Kim, R. V. Ulijn, W. E. Bentley, G. F. Payne, *Adv. Funct. Mater.* **2011**, *21*, 1575.
- [22] X. H. Yang, Y. Liu, G. F. Payne, *J. Adhes.* **2009**, *85*, 576.
- [23] J. B. Guilbaud, E. Vey, S. Boothroyd, A. M. Smith, R. V. Ulijn, A. Saiani, A. F. Miller, *Langmuir* **2010**, *26*, 11297.
- [24] R. J. Williams, A. M. Smith, R. Collins, N. Hodson, A. K. Das, R. V. Ulijn, *Nat. Nanotechnol.* **2009**, *4*, 19.
- [25] M. W. L. Popp, H. L. Ploegh, *Angew. Chem.- nt. Ed.* **2011**, *50*, 5024.
- [26] N. Shimba, Y. Yokoyama, E. Suzuki, *J. Agric. Food Chem.* **2002**, *50*, 1330.
- [27] K. Yokoyama, N. Nio, Y. Kikuchi, *Appl. Microbiol. Biotechnol.* **2004**, *64*, 447.
- [28] Y. Zhu, J. Tramper, *Trends Biotechnol.* **2008**, *26*, 559.
- [29] A. Paguirigan, D. J. Beebe, *Lab Chip* **2006**, *6*, 407.
- [30] A. L. Paguirigan, D. J. Beebe, *Nat. Protocols* **2007**, *2*, 1782.
- [31] C. W. Yung, L. Q. Wu, J. A. Tullman, G. F. Payne, W. E. Bentley, T. A. Barbari, *J. Biomed. Mater. Res. Part A* **2007**, *83A*, 1039.
- [32] T. H. Chen, H. D. Embree, E. M. Brown, M. M. Taylor, G. F. Payne, *Biomaterials* **2003**, *24*, 2831.
- [33] M. K. McDermott, T. H. Chen, C. M. Williams, K. M. Markley, G. F. Payne, *Biomacromolecules* **2004**, *5*, 1270.
- [34] E. P. Broderick, D. M. O'Halloran, Y. A. Rochev, M. Griffin, R. J. Collighan, A. S. Pandit, *J. Biomed. Mater. Res. Part B* **2005**, *72B*, 37.
- [35] A. Seitz, F. Schneider, R. Pasternack, H. L. Fuchsbauer, N. Hampp, *Biomacromolecules* **2001**, *2*, 233.
- [36] N. Kamiya, S. Doi, J. Tominaga, H. Ichinose, M. Goto, *Biomacromolecules* **2005**, *6*, 35.
- [37] N. Kamiya, T. Tanaka, T. Suzuki, T. Takazawa, S. Takeda, K. Watanabe, T. Nagamune, *Bioconjugate Chem.* **2003**, *14*, 351.
- [38] T. Tanaka, N. Kamiya, T. Nagamune, *Bioconjugate Chem.* **2004**, *15*, 491.
- [39] T. Tanaka, N. Kamiya, T. Nagamune, *FEBS Lett.* **2005**, *579*, 2092.
- [40] J. Tominaga, N. Kamiya, S. Doi, H. Ichinose, T. Maruyama, M. Goto, *Biomacromolecules* **2005**, *6*, 2299.
- [41] X. H. Yang, X. W. Shi, Y. Liu, W. E. Bentley, G. F. Payne, *Langmuir* **2009**, *25*, 338.
- [42] K. Yoshimura, M. Terashima, D. Hozan, T. Ebato, Y. Nomura, Y. Ishii, K. Shirai, *J. Agric. Food Chem.* **2000**, *48*, 2023.
- [43] S. H. Hsu, A. M. Jamieson, *Polymer* **1993**, *34*, 2602.
- [44] E. K. Johnson, D. J. Adams, P. J. Cameron, *J. Am. Chem. Soc.* **2010**, *132*, 5130.
- [45] T. Liebmann, S. Rydholm, V. Akpe, H. Brismar, *BMC Biotechnol.* **2007**, *7*, 88.
- [46] Q. M. Zhou, Q. J. Xie, Y. C. Fu, Z. H. Su, X. Jia, S. Z. Yao, *J. Phys. Chem. B* **2007**, *111*, 11276.
- [47] B. D. Larsen, D. H. Christensen, A. Holm, R. Zillmer, O. F. Nielsen, *J. Am. Chem. Soc.* **1993**, *115*, 6247.
- [48] J. De Gelder, K. De Gussem, P. Vandenabeele, L. Moens, *J. Raman Spectrosc.* **2007**, *38*, 1133.
- [49] A. M. Smith, R. F. Collins, R. V. Ulijn, E. Blanch, *J. Raman Spectrosc.* **2009**, *40*, 1093.
- [50] D. A. Buttry, M. D. Ward, *Chem. Rev.* **1992**, *92*, 1355.
- [51] T. H. Chen, D. A. Small, M. K. McDermott, W. E. Bentley, G. F. Payne, *Biomacromolecules* **2003**, *4*, 1558.
- [52] Y. Cheng, C.-Y. Tsao, H.-C. Wu, X. Luo, J. L. Terrell, J. Betz, G. F. Payne, W. E. Bentley, G. W. Rubloff, *Adv. Funct. Mater.* **2012**, *22*, 51.
- [53] K. B. Xavier, B. L. Bassler, *Nature* **2005**, *437*, 750.
- [54] L. Hall-Stoodley, J. W. Costerton, P. Stoodley, *Nat. Rev. Microbiol.* **2004**, *2*, 95.
- [55] S. Hooshangi, W. E. Bentley, *Curr. Opin. Biotechnol.* **2008**, *19*, 550.
- [56] C. M. Waters, B. L. Bassler, *Annu. Rev. Cell Dev. Biol.* **2005**, *21*, 319.
- [57] J. S. Dickschat, *Nat. Prod. Rep.* **2010**, *27*, 343.
- [58] W. Galloway, J. T. Hodgkinson, S. D. Bowden, M. Welch, D. R. Spring, *Chem. Rev.* **2011**, *111*, 28.
- [59] V. C. Kalia, H. J. Purohit, *Crit. Rev. Microbiol.* **2011**, *37*, 121.
- [60] K. R. Hardie, K. Heurlier, *Nat. Rev. Microbiol.* **2008**, *6*, 635.
- [61] Y. Irie, M. R. Parsek, in *Bacterial Biofilms*, Vol. 322 (Ed: T. Romeo), Springer Verlag, Berlin **2008**, 67.
- [62] G. D. Geske, J. C. O'Neill, D. M. Miller, M. E. Mattmann, H. E. Blackwell, *J. Am. Chem. Soc.* **2007**, *129*, 13613.
- [63] C. A. Lowery, T. Abe, J. Park, L. M. Eubanks, D. Sawada, G. F. Kaufmann, K. D. Janda, *J. Am. Chem. Soc.* **2009**, *131*, 15584.
- [64] C. A. Lowery, J. Park, G. F. Kaufmann, K. D. Janda, *J. Am. Chem. Soc.* **2008**, *130*, 9200.
- [65] K. Kamaraju, J. Smith, J. X. Wang, V. Roy, H. O. Sintim, W. E. Bentley, S. Sukharev, *Biochemistry* **2011**, *50*, 6983.
- [66] V. Roy, J. A. I. Smith, J. X. Wang, J. E. Stewart, W. E. Bentley, H. O. Sintim, *J. Am. Chem. Soc.* **2010**, *132*, 11141.
- [67] X. M. Li, S. Chu, V. A. Feher, M. Khalili, Z. Nie, S. Margosiak, V. Nikulin, J. Levin, K. G. Sprankle, M. E. Tedder, R. Almasy, K. Appelt, K. M. Yager, *J. Med. Chem.* **2003**, *46*, 5663.
- [68] S. Raina, D. De Vizio, M. Odell, M. Clements, S. Vanhulle, T. Keshavarz, *Biotechnol. Appl. Biochem.* **2009**, *54*, 65.
- [69] X. Xue, G. Pasparakis, N. Halliday, K. Winzer, S. M. Howdle, C. J. Cramphorn, N. R. Cameron, P. M. Gardner, B. G. Davis, F. Fernández-Trillo, C. Alexander, *Angew. Chem. Int. Ed.* **2011**, *50*, 9852.
- [70] E. V. Piletska, G. Stavroulakis, K. Karim, M. J. Whitcombe, I. Chianella, A. Sharma, K. E. Eboigbodin, G. K. Robinson, S. A. Piletsky, *Biomacromolecules* **2010**, *11*, 975.
- [71] B. M. M. Ahmer, *Mol. Microbiol.* **2004**, *52*, 933.
- [72] L. Wang, Y. Hashimoto, C. Y. Tsao, J. J. Valdes, W. E. Bentley, *J. Bacteriol.* **2005**, *187*, 2066.
- [73] K. B. Xavier, B. L. Bassler, *J. Bacteriol.* **2005**, *187*, 238.
- [74] C. Y. Tsao, S. Hooshangi, H. C. Wu, J. J. Valdes, W. E. Bentley, *Metab. Eng.* **2010**, *12*, 291.
- [75] M. B. Jones, R. Jani, D. C. Ren, T. K. Wood, M. J. Blaser, *J. Infect. Dis.* **2005**, *191*, 1881.
- [76] T. K. Wood, *Environ. Microbiol.* **2009**, *11*, 1.
- [77] G. F. Kaufmann, J. Park, K. D. Janda, *Expert Opin. Biol. Ther.* **2008**, *8*, 719.
- [78] J. A. Gutierrez, T. Crowder, A. Rinaldo-Matthis, M. C. Ho, S. C. Almo, V. L. Schramm, *Nat. Chem. Biol.* **2009**, *5*, 251.
- [79] D. A. Higgins, M. E. Pomianek, C. M. Kraml, R. K. Taylor, M. F. Semmelhack, B. L. Bassler, *Nature* **2007**, *450*, 883.
- [80] R. Le Berre, S. Nguyen, E. Nowak, E. Kipnis, M. Pierre, F. Ader, R. Courcol, B. P. Guery, K. Faure, G. Pyopneumagen, *Clin. Microbiol. Infect.* **2008**, *14*, 337.
- [81] L. Q. Wu, H. M. Yi, S. Li, G. W. Rubloff, W. E. Bentley, R. Ghodssi, G. F. Payne, *Langmuir* **2003**, *19*, 519.
- [82] E. Kim, Y. Liu, X. W. Shi, X. H. Yang, W. E. Bentley, G. F. Payne, *Adv. Funct. Mater.* **2010**, *20*, 2683.





**Scheme S1.** The construct for glutamine and lysine-tagged proteins



The gene for EGFP-lys was prepared by PCR amplification of an EGFP template (pET28-a(+)-GlnEK-GFP)<sup>[1]</sup> using primers EGFP-F and EGFP-lysR (**Table S2**). The sequence was inserted into pET200 using a Champion™ pET200 Directional TOPO® Expression Kit (Invitrogen). The plasmid was transformed into BL21 Star™ (DE3) One Shot® *E. coli* (Invitrogen) for protein expression.

In order to express the AI-2-synthesizing enzymes Pfs and LuxS with 5 glutamine tag (5 × Gln) or 7 lysine tag (7 × Lys), four plasmids were constructed. The genes encoding Pfs and LuxS were specifically amplified from the template plasmids pTrcHis-pfs and pTrcHis-luxS<sup>[3]</sup> by PCR using the primers listed in Table S2. The PCR products were inserted into the backbone vector pTrcHisA (Invitrogen) using XhoI and EcoRI restriction site. The plasmids were transformed into BL21 electrical competent cells.

**Table S2.** Oligonucleotide primers used in this study

Name	Sequence	Relevant description
EGFP-F	CACCATGGT GAGCAAGGCGAGGAG	Upstream primer for cloning <i>egfp</i> with a 5'-CACC sequence for directional cloning into pET200
EGFP-LysR	TTACTTTTTCTCTTTTTCTTTTTCTTTGTACAGCTC GTCCATGCCGAGAGTG	Downstream primer for cloning <i>egfp</i> with 7-lysine tag from pET28-a(+)-GlnEK-GFP <sup>[1]</sup>
PfsF	GGCAACTCGAGATGAAAATCGGCATCATTGGTGTC	Upstream primer for cloning <i>pfs</i> with 5 glutamine tag or 7 lysine tag from pTrcHis-pfs
PfsGln5R	GCCTTGAATTCTATTGCTGTTGCTGCTGGCCATGTGCAA GTTTCTGC	Downstream primer for cloning <i>pfs</i> with 5 glutamine tag from pTrcHis-pfs
PfsLys7R	GCCTTGAATTCTATTTTTCTTCTTTTTCTTTTTGCCATGT GCAAGTTTCTGC	Downstream primer for cloning <i>pfs</i> with 7 lysine tag from pTrcHis-pfs
LuxSF	GGCAACTCGAGATGCCGTTGTTAGATAGCTTCAC	Upstream primer for cloning <i>luxS</i> with 5 glutamine tag or 7 lysine tag from pTrcHis-luxS
LuxSGln5R	GCCTTGAATTCTATTGCTGTTGCTGCTGGATGTGCAGTT CCTGCAAC	Downstream primer for cloning <i>luxS</i> with 5 glutamine tag from pTrcHis-luxS
LuxSLys7R	GCCTTGAATTCTACTTTTTCTTCTTTTTCTTTTTGATGTG CAGTTCTGCAAC	Downstream primer for cloning <i>luxS</i> with 7 lysine tag from pTrcHis-luxS

The proteins of interest were overexpressed under 1 mM IPTG induction as cell densities were grown at OD<sub>600</sub> = 0.4~0.6 under 37 °C. The cells were harvested after 6 h induction by centrifugation at 14000 Xg under 4 °C for 20 min. After lysis by BugBuster solution (Novagen) at room temperature for 40 min, the soluble cell extracts were mixed with Co<sup>2+</sup> affinity resin (BD TALON™, BD Biosciences), and the bound target proteins on the Co<sup>2+</sup> were washed by phosphate buffer (pH=7.4) (Sigma) for three times to remove non-specifically bound proteins. The purified proteins were eluted by elution buffer (125 mM imidazole in phosphate buffer, pH = 7.4) for further experiments.

Enzymatic activity of 5 glutamine and 7 lysine tagged Pfs and LuxS was confirmed using an assay reported by Surette and Bassler,<sup>[4]</sup> to indicate the presence of the enzymatic product autoinducer-2 (AI-2). The purified enzymes were mixed in various combinations with a substrate *S*-adenosyl-homocysteine (SAH). After 6 h of incubation at 37 °C, the protein content of each solution was extracted with chloroform, and each aqueous phase was isolated for the assay. Activity was confirmed by detecting the presence of autoinducer-2 in all solutions that had incubated with both Pfs and LuxS enzymes.

**References**

- [1] X. H. Yang, X. W. Shi, Y. Liu, W. E. Bentley, G. F. Payne, *Langmuir* **2009**, *25*, 338-344.
- [2] C. Y. Tsao, S. Hooshangi, H. C. Wu, J. J. Valdes, W. E. Bentley, *Metab. Eng.* **2010**, *12*, 291-297.
- [3] C. Y. Tsao, L. A. Wang, Y. Hashimoto, H. M. Yi, J. C. March, M. P. DeLisa, T. K. Wood, J. J. Valdes, W. E. Bentley, *Appl. Environ. Microbiol.* **2011**, *77*, 2141-2152.
- [4] M. G. Surette, B. L. Bassler, *Proc. Natl. Acad. Sci. USA* **1998**, *95*, 7046-7050.